

*Biochemistry*. Author manuscript; available in PMC 2012 June 12.

Published in final edited form as:

Biochemistry. 2010 May 18; 49(19): 4138-4146. doi:10.1021/bi902114m.

# Conformational consequences of ionization of Lys, Asp and Gluburied at position 66 in staphylococcal nuclease †

**Daniel A. Karp**, **Mary R. Stahley**<sup>‡</sup>, and **García-Moreno E. Bertrand**<sup>\*</sup> Department of Biophysics, The Johns Hopkins University, 3400 N. Charles St., Baltimore, MD 21218

## **Abstract**

The pK<sub>a</sub> values measured previously for the internal Lys-66, Asp-66 and Glu-66 in variants of a highly stable form of staphylococcal nuclease are shifted by as many as 5 p $K_a$  units relative to normal  $pK_a$  values in water. These shifts cannot be reproduced with continuum electrostatics calculations with static structures unless the protein is treated with high dielectric constants near 10. These high apparent dielectric constants are inconsistent with the highly hydrophobic microenvironments of the ionizable moieties in crystal structures. To examine the origins of these high apparent dielectric constants we showed that the p $K_a$  of these internal residues are sensitive to the global stability of the protein; the shifts tend to be smaller in less stable forms of nuclease. This implies that the apparent dielectric constants reported by these internal ionizable groups are high because they reflect conformational reorganization coupled to their ionization. To detect this directly, acid/base titrations monitored with Trp fluorescence, near-UV and far-UV CD spectroscopy were performed on variants with Lys-66, Glu-66 or Asp-66 in background proteins with different stability. Conformational reorganization coupled to the ionization of the internal groups was spectroscopically detectable, especially in the less stable background proteins. The data show that to improve the accuracy of structure-based  $pK_a$  calculations of internal groups the calculations will have to treat explicitly all structural reorganization coupled to ionization. The data also suggest a novel approach to mapping the folding free energy landscape of proteins by using internal ionizable groups to stabilize partially unfolded states.

## **Keywords**

Protein dielectric constant; self-energy; hydration; buried ionizable group; electrostatics

Internal ionizable groups in proteins are central to key biochemical processes such as catalysis (1, 2),  $H^+$  transport (3), e- transfer (4), and ion (5) and water homeostasis (6). To describe the structural basis of biological energy transduction it is necessary to understand the molecular determinants of  $pK_a$  values of internal ionizable groups, and to quantify the effects of internal charges on protein stability and conformation. Here we examine these issues in staphylococcal nuclease (SNase), a small enzyme that is uniquely well suited for this purpose.

Val-66, one of the residues that constitute the main hydrophobic core of SNase, has been replaced previously with Lys (7–9), Asp (10), and Glu (11). The internal Lys-66, Asp-66 and Glu-66 titrate with highly perturbed  $pK_a$  values shifted by as many as 5  $pK_a$  units in the

<sup>&</sup>lt;sup>†</sup>This work was supported by NIH grant GM-061597 to B.G-M.E.

<sup>\*</sup>Corresponding Author: Bertrand García-Moreno, Department of Biophysics, The Johns Hopkins University, 3400 N. Charles St., Baltimore, MD 21218, Phone: (410) 516-4497, Fax: (410) 516-4118, bertrand@jhu.edu.

<sup>\*</sup>Current address: Department of Pharmacology and Molecular Sciences, Johns Hopkins University School of Medicine

direction that favors the neutral state (i.e. elevated for Asp and Glu, depressed for Lys). The direction of the shifts in  $pK_a$  suggests that the interior of SNase is neither as polar nor as polarizable as water. This is consistent with the crystal structures of the variants with V66K, V66D and V66E, where the ionizable groups of Lys-66, Asp-66 or Glu-66 are internal, buried approximately 10 Å from bulk solvent in a hydrophobic pocket, far from other charges or polar atoms of the protein (7–11).

Structure-based calculations with continuum electrostatics methods suggest that the p $K_a$ values of these internal groups are perturbed because the dehydration experienced by the ionizable groups in their deeply buried positions is not compensated by interactions with polar groups, surface charges, or by the buried water molecules that are observed in some crystal structures (10–12). To reproduce the experimental p $K_a$  values in these calculations the protein has to be treated with a dielectric constant of approximately 10 (7–11). These apparent dielectric constants are not to be confused with the real dielectric constant of the protein. They are model dependent quantities without precise structural or physical meaning, intended to capture implicitly all factors that are not dealt with explicitly or correctly in the calculations (13). Despite their imprecise physical meaning, they are useful to gauge the magnitude of the net polarizability experienced by an internal ionizable group. The high values of the apparent dielectric constant reported by Lys-66, Asp-66 and Glu-66 suggest that the interior of SNase is highly polarizable, but this is not consistent with the hydrophobic nature of the microenvironments surrounding these ionizable moieties in the crystal structures. The structural origins of the high apparent dielectric constant reported by these ionizable groups are not known.

The dielectric properties of a material are determined by polarization and relaxation processes. For water at 298 K, electronic polarization is responsible for the high-frequency dielectric constant of 3 (14), whereas its overall dielectric constant of 78.5 is governed by the relaxation of water molecules in the electrostatic field. The interior of proteins is usually neither as polar nor as polarizable as water; therefore, the magnitude of the dielectric effect inside a protein is expected to be lower than that of water. The low dielectric constants of 2 to 4 measured experimentally with dry protein powders are determined primarily by electronic polarization (15–17). Contributions from dipolar relaxation processes cannot be measured experimentally with dry protein powders because water is required to activate dynamic processes, and in its presence, the dielectric properties measured are those of water, not of protein.

All the factors that affect the  $pK_a$  of an internal group can, in principle, contribute towards the apparent dielectric constant reported by said group(18). Chief among these factors are interactions with surface charges and with fixed permanent dipoles (19), dipole relaxation (20), the reaction field from polarization of bulk water, and water penetration (12). However, when the ionization of an internal group triggers significant dipole relaxation or large-scale structural reorganization, all other factors are less relevant and dipole relaxation or structural reorganization become the dominant contribution to the apparent dielectric effect and to the  $pK_a$ . For this reason, it is of interest to examine the extent to which the high apparent dielectric constant reported by Lys-66, Asp-66 and Glu-66 in SNase reflects conformational reorganization coupled to the ionization of the internal groups.

Initial evidence that the ionization of these internal groups triggers subtle structural reorganization came from recent demonstration that the ionization of Asp-66 in a highly stable form of SNase induces a small loss of intensity in the far-UV CD signal, consistent with the loss of  $\alpha$ -helical content (10). We speculated that the ionization of Asp-66 triggers the unwinding of one turn of  $\alpha$ -helix. This would be sufficient to expose the previously buried carboxylic group of Asp-66 to bulk water and to normalize its p $K_a$ . This was not

observed clearly in previous studies with Glu-66 (11) or Lys-66 (7) in a highly stable forms of SNase. Here we show that the  $pK_a$  values of the ionizable groups at position 66 in SNase are affected by the global stability of the protein and that the ionization of the internal groups triggers conformational reorganization detectable with Trp fluorescence and CD spectroscopy. The approach involved comparison of the consequences of ionization of Lys-66, Asp-66 and Glu-66 in two different forms of SNase with stabilities different by 4 kcal/mol. The studies show that the high apparent dielectric constants reported by Lys-66, Asp-66 and Glu-66 reflect a conformational transition coupled to the ionization of the internal groups. Besides clarifying the structural meaning of the high apparent dielectric constant reported by these internal groups, these experiments also draw attention to the limitations inherent to  $pK_a$  calculations with continuum methods that use a single, static structure. Computational methods that do not treat explicitly the coupling between the ionization of internal groups and conformational reorganization are likely to yield inaccurate estimates of  $pK_a$  values.

## MATERIALS AND METHODS

## Staphylococcal nuclease

The Quickchange kit from Stratagene (La Jolla, CA) was used to make the substitutions V66K, V66D or V66E in two stable forms of staphylococcal nuclease (SNase), one known as PHS after the three substitutions used to engineer it (P117G, H124L, and S128A), and a second one known as  $\Delta$ +PHS (PHS with additional G50F and V51N substitutions and a 44–49 deletion). All mutagenesis was performed with the  $\lambda$  pL9 plasmid. Proteins were expressed and purified by the method of Shortle and Meeker (21) as modified by Byrne et al (22). Protein concentration was determined using an extinction coefficient of  $1.46\times10^4$  M<sup>-1</sup>cm<sup>-1</sup>, determined using the method of Gill and von Hippel (23). Background and variant proteins were treated with the same extinction coefficient.

#### pH titrations monitored by fluorescence and CD

The acid/base titrations monitored by changes in intrinsic fluorescence were performed with an AVIV ATF-105 automated titration fluorometer (Aviv Inc, Lakeland, NJ). The titrations that monitored changes in CD were performed with an AVIV 215 CD spectrometer (Aviv Inc, Lakeland, NJ). All data were collected at 25 °C in 100 mM KCl following protocols that have been described previously(24). The only difference between the protocols used with wild type SNase and with the variants with internal ionizable groups is that the delay times between the delivery of consecutive doses of titrant in the automated acid/base unfolding experiments were longer for variants in both  $\Delta$ +PHS and PHS backgrounds. Delay times of 2 minutes for PHS and its variants, and 5 minutes for  $\Delta$ +PHS and its variants, were used to allow the system to reach equilibrium. This delay corresponds to 7 lifetimes in the decay of the fluorescence signal following a pH jump from pH 7 to the pH at the midpoint of the unfolding transitions. The experiments monitoring intrinsic fluorescence and CD at 222 nm were performed with a protein concentration of approximately 50 µg/ml. Experiments that monitored CD at 275 nm were performed with approximately 500 µg/ml. The buffers used in acid titrations monitored by fluorescence consisted of 5 mM MES, 5 mM HEPES and 100 mM KCl. In the base titrations the buffer was 5 mM HEPES with 100 mM KCl. The titrations monitored by CD were performed with a buffer consisting of 100 mM KCl and 5 mM each of MES, HEPES, TAPS, CHES and CAPS. Samples were titrated with 0.3 N HCl or KOH. All buffers and titrants were from Sigma (St. Louis, MO). The analysis of acid/base titrations to obtain the midpoints of the unfolding transitions (pH<sub>mid</sub>) or to describe the steepness of the transition ( $\Delta v_{H+}$ ) was performed by nonlinear least squares fit of two- or three-state models of the unfolding process to the data, using the equations described previously (10).

#### Stability measurements by chemical denaturation

The Gibbs free energy of unfolding ( $\Delta G^{\circ}_{H2O}$ ) was measured using the intrinsic fluorescence of Trp-140 to monitor unfolding as described previously (24). GdmCl (UltraPure grade Invitrogen Life Technologies, CA) was used as a denaturant. All measurements were performed with ATF-105 automated fluorometer (Aviv Inc, Lakeland, NJ). In the PHS background, in the transition region, five minutes were allowed for equilibration following the addition of titrant. In the  $\Delta$ +PHS background the delay time was between forty to eight minutes. Protein concentration in these experiments was 50 µg/ml. The buffers varied according to the pH of the experiment. They consisted of 100 mM NaCl with 25 mM each of sodium acetate for pH 4 to 5.5, MES for pH 5.5 to 6.5, HEPES for pH 7 to 8, TAPS for pH 8 to 9, CHES for pH 9 to 10, and CAPS for pH 10 to 11. At the higher pH values, it is difficult to regulate the pH during the titration because GdmCl shifts the p $K_a$  of the buffer. The pH of the solutions at high pH drifted by as much as 0.1 pH units over the course of a titration. At the pH values where the GdmCl titration curve did not reach a native state baseline, the fluorescence value obtained for the native state at other pH values was used to analyze the data to obtain the thermodynamic parameters. The pH of the samples was always checked at the end of each experiment. The final concentration of GdmCl was also measured at the end of each experiment by refractometry. All data were collected at 25 °C.

#### Potentiometric H<sup>+</sup> titrations

The procedure for the measurement of  $H^+$  titration curves of SNase with direct potentiometric methods has been presented elsewhere (7, 11, 24). The data were obtained with protein concentrations of 3 to 4 mg/ml. The protein and water samples were titrated with HCl or KOH of approximately 0.15 N. Reversibility of the titration curves was tested routinely. All titration curves were measured in triplicate. All data were collected at 25 °C in 100 mM KCl. The data were treated by linear interpolation.

## X-ray crystallography

The V66K variant of PHS nuclease was crystallized by the hanging drop vapor diffusion method at 4  $^{\circ}$ C. The reservoir solution consisted of 36.5–39% (vol/vol) 2-methyl-2,4-pentanediol and 15 % glycerol in 25 mM potassium phosphate buffer, pH 7.0. Two milliequivalents of the inhibitor pdTp and 3 milliequivalents of CaCl<sub>2</sub> were added to 9.6 mg/ml protein solution before mixing with an equal volume of reservoir solution. pdTp was synthesized in our laboratory (10). Crystals of PHS/V66K appeared in 1–2 weeks at 4  $^{\circ}$ C.

Diffraction data were collected at three conditions. Two data sets were collected at 100 K, at pH 7 and 4.7, and the third was collected at 298 K at pH 5. Data were collected from a single crystal at each condition using an R-AXIS IV image plate detector (MSC, The Woodlands, TX). To obtain data at pH 4.7, crystals grown at pH 7 were transferred into drops of synthetic mother liquor with successively lower pH values. Three transfers were performed to achieve a pH of 4.7. For the structure obtained at pH 5, the crystal was transferred only twice. This procedure minimized the cracking of crystals. For the low temperature structure, the crystal was mounted in a thin loop, with the crystallization buffer as cryosolvent, and flash frozen under a stream of nitrogen at 100 K. For the room temperature structure the crystal was mounted in a thin-walled glass capillary in equilibrium with the well solution. Crystals for all three data sets were found to be isomorphous to those of PHS/V66E (11) and this structure was used as an initial phasing model. Refinement for each structure was carried out using the programs CNS and O(25, 26). For the crystal at pH 7, data were collected in the resolution range 29.0–1.95 Å. For the crystal at pH 4.7, data were collected in the resolution range 24.0-2.0 Å and the structure was refined to a final R value of 19.9% and an R<sub>free</sub> of 23.57%. For the structure at pH 5 data were collected in the resolution range 27.0-2.2 Å and the structure was refined to a final R value of 18.76% and a

final  $R_{free}$  of 23.06%. The electron density for the side chain of Lys-66 was fully visible in the electron density maps at pH 7, mostly visible at pH 5, and totally unresolvable from C $\beta$  to the amino moiety at pH 4.7.

## **RESULTS**

The goal of this study was to examine structural consequences of the ionization of the internal Lys-66, Asp-66 and Glu-66 in SNase, with the intent of determining if conformational reorganization coupled to their ionization was responsible for the high apparent dielectric constants necessary to reproduce the p $K_a$  of these groups with continuum electrostatics calculations. To this end, we compared the energetics of ionization of Lys-66, Asp-66 and Glu-66 in two different forms of SNase engineered to be more stable than the wild type protein. One of these proteins, referred to as  $\Delta$ +PHS SNase, has a deletion from 44 to 49 and five substitutions (P117G, H124A, S128L, G50F, V51N) relative to the wild type protein. The stability ( $\Delta G^{\circ}_{H2O}$ ) of  $\Delta$ +PHS SNase at pH 7 and 100 mM ionic strength is 11.8 kcal/mol (10). The other form of SNase used in this study is known as PHS SNase after the three substitutions (P117G, H124A, S128L) used to engineer it. PHS has a stability of 8 kcal/mol at pH 7, 298 K, 100 mM ionic strength. The p $K_a$  of Lys-66, Asp-66 and Glu-66 were reported previously (7, 8, 10, 11), but the published data were not sufficient for comparison of the properties of the different internal ionizable groups in background proteins with different stability.

The  $\Delta$ +PHS protein was used in the original studies of p $K_a$  values of internal ionizable residues precisely because of its high stability, to counterbalance the destabilization of the protein when core hydrophobic positions are substituted with ionizable ones, and to maximize the range of pH over which the proteins are stable (27). By using the less stable PHS background protein we hoped to unmask conformational transitions coupled to the ionization of the internal groups.

#### Stability measured by chemical denaturation

The thermodynamic stability ( $\Delta G^{\circ}_{H2O}$ ) of PHS and  $\Delta+PHS$  nuclease and of their V66D and V66E variants, measured over a range of pH values, are shown in Figure 1A. The shape of the pH dependence of stability of the variants with Asp-66 and Glu-66 is characteristic of proteins with carboxylic groups with p $K_a$  value shifted towards values higher than the normal p $K_a$  of 4.0 and 4.5 for Asp and Glu in water, respectively. The direction of the shifts in p $K_a$  is consistent with a preference for the neutral state when the groups are buried in the hydrophobic interior of the folded protein.

The stabilities of the PHS and  $\Delta$ +PHS proteins are roughly parallel over a wide range of pH, as are the two curves for the corresponding variants with Asp-66 or Glu-66. For example, at pH 7 the difference in  $\Delta G^{\circ}_{H2O}$  for the V66E variant in PHS and in  $\Delta$ +PHS is almost 4 kcal/mol, comparable to the difference between the PHS and  $\Delta$ +PHS proteins at this pH. The difference ( $\Delta\Delta G^{\circ}_{H2O}$ ) in  $\Delta G^{\circ}_{H2O}$  for variants with either V66D or V66E substitutions in the PHS and in the  $\Delta$ +PHS background (i.e. ( $\Delta G^{\circ}_{H2O}$  of the variant minus  $\Delta G^{\circ}_{H2O}$  for the background) also superimpose very well (Fig. 1B). This implies that the substitutions at Val-66 have comparable impact on  $\Delta G^{\circ}_{H2O}$  in the two different background proteins.

## pKa of Lys-66, Glu-66, and Asp-66

The shape of the  $\Delta\Delta G^{\circ}_{H2O}$  vs pH curves in Figure 1B reflects differences in the p $K_a$  values of Asp-66 and Glu-66 in the native and in the denatured states. The two regions where these curves exhibit a change in curvature have information about p $K_a$  values. The use of linkage thermodynamic relationships to obtain p $K_a$  values for the internal ionizable groups by

analysis of these curves was described previously (9, 10).  $pK_a$  values were also measured with direct potentiometric methods, as described previously (8). These experiments involve measurement of  $H^+$  binding/release of the background protein and of the variant with the internal ionizable group, as illustrated for the PHS/V66D variant in Figure 2. This approach works only if the shift in the  $pK_a$  of the internal group is significant, and if the substitution does not affect the  $pK_a$  values of other groups, as is the case with the variants of interest to this study. The  $H^+$  titration curves of PHS and of its V66D variant (insert, Fig. 2) show that at high pH values more  $H^+$  are released by the PHS protein than by the PHS/V66D variant, consistent with the ionization of Asp-66 with an apparent  $pK_a$  value near 8.

The p $K_a$  values measured with the two different equilibrium thermodynamic methods (linkage of  $\Delta\Delta G^{\circ}_{H2O}$  vs. pH or potentiometric measurements) are comparable (Table 1). The differences between the p $K_a$  of Asp-66 and Lys-66 in the different background proteins are noteworthy. The shift in the p $K_a$  of Asp-66 and Lys-66 is smaller by almost a full p $K_a$  unit in the less stable PHS form of SNase than in the  $\Delta$ +PHS protein. This dependence of the p $K_a$  values on the stability of the background protein is consistent with the ionization of these groups being coupled to local or global unfolding. In the case of Glu-66 the p $K_a$  values measured in the two different background proteins were comparable (Table 1). This does not necessarily exclude coupling between the ionization of Glu-66 and structural reorganization, but it does imply that the magnitude of the shift in the p $K_a$  of this group was not limited by the global stability of the protein.

## Detection of conformational changes with Trp fluorescence and CD spectroscopy

Acid/base titrations monitored with three different types of spectroscopic signals were used to detect conformational reorganization coupled to the ionization of internal groups: (1) intrinsic fluorescence of Trp-140, which is known to be an excellent reporter of global unfolding of SNase (21, 28, 29); (2) far-UV CD at 222 nm, which reports primarily on the  $\alpha$ -helical contents of the protein, with some contribution from  $\beta$ -sheets; (3) near-UV CD at 275 nm, which reports primarily on the microenvironments of the aromatic residues, which are abundant in SNase.

Large differences were observed in the pH titrations of the PHS and  $\Delta$ +PHS proteins monitored with the different spectroscopic probes (Fig 3). A broad pre-denaturational transition was observed for these two proteins at pH values above 9 by both fluorescence and near-UV CD (Fig. 3A and 3B). In the titrations monitored by Trp fluorescence (black open and solid red circles) this likely reflects contributions from tyrosinate, which begins to be formed in this pH range and which is fluorescent (7). In the near-UV CD this predenaturational transition at high pH might also be related to changes in the conformational state of tyrosine residues. The steep cooperative transition reported for both proteins by all three probes at high pH corresponds to the base-unfolding transition; the midpoint of this transition reported by the different probes is the same (Table 2).

The acid-base titrations of the V66K, V66D and V66E variants in the  $\Delta$ +PHS background (Fig. 3A–C, green curves) showed evidence of conformational reorganization coincident with the ionization of the internal ionizable groups. This was observed originally with the  $\Delta$ +PHS/V66D variant by far-UV CD at 222 nm (10); this prompted the reexamination of the behavior of variants with Glu-66 and Lys-66, for which the effect had gone unnoticed in previous studies with Trp fluorescence. The titration of  $\Delta$ +PHS/V66E monitored by fluorescence and by near UV CD spectra showed no evidence of a conformational transition in the range of pH 8 to 10 where Glu-66 with a p $K_a$  of 9.1 becomes charged. In contrast, titration monitored by far-UV CD showed evidence for the disruption of  $\alpha$ -helix and perhaps even  $\beta$ -sheet concomitant with the ionization of Glu-66. In the  $\Delta$ +PHS/V66K protein, the coincidence between the pH titration monitored by intrinsic fluorescence and by

far-UV CD, and their similarity with the titration of the  $\Delta$ +PHS protein monitored by Trp fluorescence, obscured the conformational transition. The conformational change coupled to the ionization of Lys-66 with a p $K_a$  of 5.6 was more obvious when the titrations of  $\Delta$ +PHS/V66K and  $\Delta$ +PHS were compared in the far-UV and near-UV CD.

The conformational changes coupled to the ionization of the internal ionizable groups were amplified and more obvious when the titrations were monitored in the variants engineered using the less stable PHS background protein (Fig. 3A-C, blue curves). This was particularly clear in the pH titrations of the PHS/V66K and PHS/V66D proteins. In the case of PHS/V66K (Fig. 3C, blue curves), the three spectroscopic signals report a somewhat biphasic, non-cooperative unfolding, with one transition centered near the p $K_a$  values of 6.4 measured for Lys-66 in PHS nuclease, and a second acid unfolding transition at lower pH that reports on acid unfolding (Table 2). The intensity of the three spectroscopic signals decreased significantly with decreasing pH, suggesting that the ionization of Lys-66 in the PHS background disrupts the native state. The case for a conformational transition coupled to the ionization of Asp-66 in PHS/V66D (Fig. 3A, blue curves) is equally clear. The far-UV CD signal monitored a monotonic titration in the range coincident with the titration of Asp-66 with a p $K_a$  value of 8 (Table 2). The near-UV CD and the intrinsic fluorescence signals exhibited a biphasic response, with a first titration event at pH 8, coincident with the  $pK_a$  of Asp-66, and a second, well-defined titration centered near pH 10. This second titration, corresponding to global unfolding by base, was also observed in the PHS/V66E variant.

## Effects of osmolytes on p $K_a$ values

To further establish a dependence between the measured  $pK_a$  values of internal groups and the stability of the parent protein, some measurements were repeated in the presence of glycerol, which is known to stabilize the native state of SNase (30). In general, stabilizing osmolytes such as sucrose, glycerol and TMAO promote the native states of proteins because unfavorable interactions between backbone and osmolytes are minimized in this state (30).

Attempts were made to measure the p $K_a$  of Lys-66 in  $\Delta$ +PHS/V66K and of Asp-66 in PHS/ V66D by potentiometry in the presence of 4 M glycerol. The stabilizing effects of glycerol were clearly evident in the wider range of pH over which the proteins remained folded (Figure 4). Because glycerol stabilized the protein, the  $pK_a$  value of Lys-66 measured in its presence was expected to be lower than in its absence; conversely, the p $K_a$  value of Asp-66 was expected to be higher. The data were not of the same high quality as those measured in water owing to the difficulties inherent to measurements in viscous solutions in high glycerol concentrations. For this reason we did not obtain  $pK_a$  values. However, the trends that were observed are fully consistent with the notion that an agent that stabilizes the native state and which suppresses local and global unfolding leads to even greater shifts in the p $K_a$ values. The biphasic pH titration monitored by fluorescence with the PHS/V66D protein in water became nearly sigmoidal in the presence of 4 M glycerol (Figure 4), showing clearly that the conformational reorganization coupled to the ionization of Asp-66 was suppressed in the presence of a stabilizing agent. The effects of osmolytes on the p $K_a$  of Lys-66 and Asp-66 were fully consistent with the notion that the p $K_a$  values are governed by the local stability of their microenvironments and by the probability of populating locally or partially unfolded states.

## X-ray crystallography

Crystal structures have been obtained previously for variants with Lys-66 (7, 9), Asp-66 (10), or Glu-66 (11), but only under conditions of pH where these internal ionizable groups

are neutral. We have been unable to grow crystals of any of these variants under conditions of pH where the groups are presumably charged. However, crystals of PHS/V66K grown at pH 7 tolerated transfer to pH 5, where Lys-66 is likely to be charged. The transfer from high to low pH often led to the cracking of crystals, but by trial and error it eventually became possible to lower the pH of crystals without damaging them.

The structures of the V66K variant that were previously available were obtained in the wild type background (9) and in the Δ+PHS background (8) at pH 8 under cryogenic conditions. The structure of the V66K variant of PHS protein was obtained in three conditions: (1) at pH 7 under cryogenic conditions; (2) at pH 5 at room temperature; and (3) at pH 4.7 under cryogenic conditions. The conformation of the backbone of all V66K variants was nearly identical regardless of the conditions or of the background used. The only relevant observation in the structures of the V66K variant at lower pH values was that the electron density for the side chain of the internal Lys-66, which is clearly visible in maps at pH 7, could not be resolved at the lower pH values. At pH 4.75, where in solution Lys-66 is presumably fully charged, there was no density for the side chain, not even for CB. The absence of density for  $C\beta$  suggested that the backbone in this region of the protein was disordered. Additional, albeit indirect and qualitative evidence for disorder in the backbone came from comparison of the B-factors for Ca atoms in the structures obtained under cryogenic conditions at pH 7 and 4.7. In the structure at low pH, where Lys-66 is presumably charged 1, B factors were significantly higher for the region in the  $\alpha$ -helix in the vicinity of residues 66, as well as being somewhat higher in the adjacent  $\beta$ -1 strand (Fig. 5). The more substantial loss of α-helix measured by far UV-CD (Fig. 3C) was not evident in the crystals. Other cases where conformational relaxation induced by the formation of a buried charge is evident in optical spectroscopic methods but not in crystal structures have been reported (31). In the case of the structure with ionized Lys-66, three factors could have stabilized the fully folded state in the crystal and obscured the conformational relaxation observed spectroscopically. First, lattice forces in the crystal can influence the conformation of the protein and selectively stabilize the folded state relative to the fully folded one. Second, the osmotic properties of the solution used to grow crystals must stabilize the native state. Crystals were grown with MPD, which probably destabilizes SNase, but glycerol was included in the drops, which enhances the stability of SNase. Third, the crystals were grown in the presence of Ca<sup>2+</sup> and the inhibitor pdTp, which bind at the active site with high affinity and stabilize the native state significantly.

#### DISCUSSION

The very large shifts in the  $pK_a$  values of Lys-66, Glu-66 and Asp-66 in SNase relative to the normal values in water, and in the direction that favors the neutral state, imply that the microenvironment of the ionizable moieties inside the protein are not as polarizable as water. What is noteworthy is that, although the shifts in  $pK_a$  values of these residues are very large, they are actually consistent with high apparent polarizability in the protein interior (7, 10, 11), comparable to that of a material with a dielectric constants of 10. A dielectric constant of 10 is very high relative to the value of 2 to 4 measured with dry protein powders (15–17). It is in the range of dielectric constants expected from highly polar and polarizable materials. Similarly high apparent dielectric constants are reported by naturally

<sup>&</sup>lt;sup>1</sup>The p $K_a$  of Lys-66 was measured in solution but the p $K_a$  of Lys-66 when the protein is in a crystal is not known. If crystal packing affects the ability of the protein to respond to the ionization of this Lys residue, the p $K_a$  in the crystal will be affected. In fact, if crystal contacts destabilize the unfolded form or stabilize the folded form the p $K_a$  of Lys-66 could be even lower in the crystal than in solution. If this were the case, Lys-66 in the crystal at low pH might be fully or partially deprotonated. This would be consistent with the absence of more significant conformational reorganization in the crystal structure.

occurring internal ionizable groups in active sites of enzymes and in many other types of proteins (1, 2, 8, 32).

The spectroscopic data demonstrate unequivocally that the ionization of Lys-66, Asp-66 and Glu-66 in SNase triggers structural reorganization. Because the probability of structural transitions is determined by the free energy difference between the ground state and the alternative conformational state achieved when the internal ionizable groups are charged, the  $pK_a$  values of the internal ionizable groups are sensitive to the global stability of the protein. Structural reorganization was made more readily apparent by lowering modestly the stability of the background protein used to study the ionization of the internal groups. The structural changes coupled to the ionization of the internal groups appear to be subtle, leaving most of the native structure of the protein intact, especially in the more stable  $\Delta$ +PHS protein. This is consistent with the interpretation given to magnetic relaxation dispersion studies of the V66E and V66K variants of  $\Delta$ +PHS nuclease (33).

The demonstration that the ionization of an internal group is coupled to a conformational transition and dependent on the global stability of the protein used for the measurements is significant. It implies that the  $pK_a$  values of internal groups need not report on the true polarizability of their microenvironment. At least in the case of Lys-66, Asp-66 and Glu-66, their  $pK_a$  values report on local or global stability of the protein. The apparent dielectric constants obtained from these  $pK_a$  values are not interpretable in terms of dielectric permittivity proper –they reflect the dielectric breakdown of the protein.

Details of the nature of the conformational reorganization coupled to the ionization of Lys, Asp or Glu at position 66 in SNase are not known at this time. NMR spectroscopy studies are underway to examine these conformational transitions in depth. It is likely that in the conformational state stabilized by the ionization of the internal group the previously buried charged moieties are well hydrated. Based on the location of position 66 at the C terminal end of an  $\alpha$ -helix (Fig. 4) and on the characteristic loss of intensity in the far-UV CD at 222 nm where  $\alpha$ -helices contribute, we speculated (10) that the ionization of Asp-66 triggers the partial unwinding of helix-1. The structural change coupled to the ionization of Lys-66 and Glu-66 is probably similar. The spectroscopic data measured with the variants made with the  $\Delta$ +PHS background protein suggest that the conformational transition involves subtle local or sub-global rearrangement. In all cases the structural transition triggered by the ionization of the internal groups precedes a steep cooperative transition corresponding to the global acid or base unfolding. This further shows that substantial native-like structure is still present after the internal groups are charged.

The conformational transitions coupled to the ionization of internal groups observed with SNase and with other model proteins (34) is probably similar to the conformational reorganization coupled to the ionization of naturally occurring internal ionizable groups (18, 35, 36). Conformational transitions coupled to the ionization of naturally occurring internal groups are usually functionally relevant, and an important recurring motif central to energy transduction. For example, the kinetic mechanism of  $H^+$  transport in bacteriorhodopsin depends on the modulation of  $pK_a$  values through reorganization of main chain and side chain atoms inside the protein (37–39). In ATPsynthase the utilization of the protonmotive force by the FO subunit is governed by the coupling between conformational reorganization and changes in the charged state of a critical carboxylate (40). The photoactive yellow protein undergoes a substantial conformational change in response to the formation of a buried charge during its cycle of biological function (41–43). The partially unfolded state promoted by the ionization of an internal group is the form of this protein that is active in signaling. In all these cases, the ultimate goal of dissection of structure-function

relationships will involve understanding the nature of the conformational transition triggered by the ionization of an internal groups.

Demonstration that the p $K_a$  of Lys-66, Asp-66 and Glu-66 in SNase are governed by the stability and conformational reorganization of the protein has significant implications for structure-based p $K_a$  calculations. It is well known that structure-based electrostatic calculations with continuum models overestimate the magnitude of electrostatic effects in proteins (13, 44–47). The properties of internal ionizable groups are notoriously difficult to reproduce with these methods (7, 10, 13, 19, 20). At least in the case of the internal Lys-66, Asp-66 and Glu-66 in SNase, the problems stem from the inability of computational models to account for the energetic consequences of coupling between ionization of an internal residue and conformational reorganization.

The demonstration that the p $K_a$  values of some internal ionizable groups are linked to global and local stability underscores inherent limitations of continuum electrostatics calculations with static structures. The problems can be addressed through the empirical use of high dielectric constants (7, 10, 13, 19, 20), but this is a poor solution to a complex problem. More rigorous methods that employ Monte Carlo side chain repacking (48, 49) or molecular dynamics simulations (50, 51) are available. Our spectroscopic evidence showing that the conformation of the backbone changes during the titration of internal ionizable groups suggests that methods capable of sampling alternate conformations of the backbone will be necessary to study biologically important processes governed by the ionization of internal groups. A variety of novel computational methods have been proposed for these purposes (52–56). These methods attempt to calculate p $K_a$  values of internal ionizable groups by reproducing conformational transitions coupled to their ionization, as proposed originally by Warshel and co-workers in their PDLD/S-LRA algorithm (36). Doing this accurately will require calculation of the thermodynamic stability of proteins, which is still a challenging undertaking. At the very least it will be necessary to drive the protein across a free energy landscape, pushing it out of local minima, with self-consistent evaluation of free energy along the way (54).

Finally, we note that substitution of internal hydrophobic residues with ionizable ones might turn out to be a useful strategy for mapping the folding free energy landscapes of proteins. Because folding is usually highly cooperative, folding intermediates are suppressed, presently only transiently, and difficult to study. Our results suggest that by charging an internal group it is possible to stabilize partially unfolded state that can be then studied with equilibrium thermodynamic methods. We speculate that the driving force behind the partial or local unfolding promoted by the ionization of an internal group is the need for the internal charge to be hydrated. Sometimes this will be achieved by the penetration of water into the protein. Clearly, in other cases, when partially folded states in which the internal charge is hydrated are accessible, the ionization of the internal group will promote these alternative, partially folded states. Although it will be difficult to establish that these partially folded states are relevant to the protein folding reaction proper, the possibility of measuring the free energy distance between the fully folded state and many such partially unfolded states would give truly novel insight into the properties of the folding free energy landscape of proteins.

# **Acknowledgments**

This work was supported by National Institutes of Health grant GM-065197. D. A. K. acknowledges a pre-doctoral fellowship from the National Science Foundation. The authors thank Dr. Daniel G. Isom for sharing his spectroscopic data on  $\Delta$ +PHS nuclease, and Dr. Apostolos Gittis for working with D. A. K. in data collection and refinement of crystal structures.

#### **Abbreviations**

SNase Staphylococcal nuclease

CD circular dichroism

GdmCl guanidinium chloride

PHS variant of SNase with P117G, H124S, S128AΔ+PHS PHS with a 44–49 deletion, G50F and V51N

**MPD** 2-methyl-2,4-pentanediol

## **REFERENCES**

 Li Y, Kuliopulos A, Mildvan AS, Talalay P. Environments and Mechanistic Roles of the Tyrosine Residues of Δ5-3-Ketosteroid Isomerase. Biochemistry. 1993; 32:1816–1824. [PubMed: 8439542]

- 2. Czerwinski RM, Harris TK, Massiah MA, Mildvan AS, Whitman CW. The structural basis for the perturbed p*K*a of the catalytic base in 4-oxalocrotonate tautomerase: Kinetic and structural effects of mutations of Phe-50. Biochemistry. 2001; 40:1984–1995. [PubMed: 11329265]
- 3. Luecke H, Lanyi JK. Structural Clues to the Mechanism of Ion Pumping in Bacteriorhodopsin. Advances in Protein Chemistry. 2003; 63:115–130.
- 4. Parson WW, Chu ZT, Warshel A. Electrostatic control of charge separation in bacterial photosynthesis. Biochim. Biophys. Acta. 1990; 1017:251–272. [PubMed: 2196939]
- 5. Doyle DA, Cabral JM, Pfuetzner RA, Kuo A, Gulbis JM, Cohen SL, Chait BT, MacKinnon R. The Structure of the Potassium Channel: Molecular Basis of K+ Conduction and Selectivity. Science. 1998; 280:69–77. [PubMed: 9525859]
- Burykin A, Warshel A. What Really Prevents Proton Transport through Aquoporin? Charge Self-Energy versus Proton Wire Proposals. Biophysical J. 2003; 85:3696–3706.
- 7. Fitch CA, Karp DA, Lee KK, Stites WE, Lattman EE, García-Moreno EB. Experimental p*K*a values of buried residues: analysis with continuum methods and role of water penetration. Biophysical Journal. 2002; 82:3289–3304. [PubMed: 12023252]
- 8. García-Moreno EB, Dwyer J, Gittis A, Lattman E, Spencer D, Stites W. Experimental measurement of the effective dielectric in the hydrophobic core of a protein. Biophysical Chemistry. 1997; 64:211–224. [PubMed: 9127946]
- Stites WE, Gittis AG, Lattman EE, Shortle D. In a staphylococcal nuclease mutant the side-chain of a lysine replacing valine 66 is fully buried in the hydrophobic core. Journal of Molecular Biology. 1991; 221:7–14. [PubMed: 1920420]
- Karp DA, Gittis AG, Stahley MR, Fitch CA, Stites WE, García-Moreno EB. High Apparent Dielectric Constant Inside a Protein Reflects Structural Reorganization Coupled to the Ionization of an Internal Asp. Biophysical Journal. 2007; 92:2041–2053. [PubMed: 17172297]
- 11. Dwyer J, Gittis A, Karp D, Lattman E, Spencer D, Stites W, García-Moreno EB. High apparent dielectric constants in the interior of a protein reflect water penetration. Biophysical Journal. 2000; 79:1610–1620. [PubMed: 10969021]
- 12. Schlessman JL, Abe C, Gittis AG, Karp DA, Dolan MA, Garcia-Moreno EB. Crystallographic study of hydration of an internal cavity in engineered proteins with buried polar or ionizable groups. Biophys. J. 2008; 94:3208–3216. [PubMed: 18178652]
- 13. Schutz CN, Warshel A. What are the dielectric "constants" of proteins and how to validate electrostatic models? Proteins: Structure, Function, Genetics. 2001; 44:400–417.
- 14. Pethig, R. Dielectric and Electronic Properties of Biological Materials. Chichester: John Wiley and Sons; 1979.
- 15. Harvey SC, Hoekstra P. Dielectric relaxation spectra of water adsorbed on lysozyme. Journal of Physical Chemistry. 1972; 76:1987–2994.
- 16. Bone S, Pethig R. Dielectric studies of protein hydration and hydration-induced flexibility. Journal of Molecular Biology. 1985; 181:323–326. [PubMed: 2984434]

17. Bone S, Pethig R. Dielectric studies of the binding of water to lysozyme. Journal of Molecular Biology. 1982; 157:571–575. [PubMed: 7120403]

- 18. Warshel A, Sharma PK, Kato M, Parson WM. Modeling electrostatic effects in proteins. Biochimica et Biophysica Acta. 2006; 1764:1647–1676. [PubMed: 17049320]
- 19. Harms MJ, Castañeda CA, Schlessman JL, Sue GR, Isom DG, Cannon BR, García-Moreno EB. The p*K*a values of acidic and basic residues buried at the same internal location in a protein are governed by different factors. J. Mol. Biol. 2009; 389:34–47. [PubMed: 19324049]
- 20. Harms MJ, Schlessman JL, Chimenti MS, Sue GR, Damjanovic A, García-Moreno EB. A buried lysine that titrates wiht a normal pKa: Role of conformational flexibility at the protein water interface as a determinant of pKa values. Protein Science. 2008; 17:833–845. [PubMed: 18369193]
- 21. Shortle D, Meeker A. Mutant forms of staphylococcal nuclease with altered patterns of guanidine hydrochloride and urea denaturation. Proteins: Structure, Function, and Genetics, 1986; 1:81–89.
- Byrne M, Manuel R, Lowe L, Stites W. Energetic contribution of side chain hydrogen bonding to the stability of staphylococcal nuclease. Biochemistry. 1995; 34:13949–13960. [PubMed: 7577991]
- 23. Gill SC, Von Hippel PH. Calculation of protein extinction coefficients from amino acid sequences. Analytical Biochemistry. 1989; 182:319–326. [PubMed: 2610349]
- Whitten ST, García-Moreno EB. pH dependence of stability of staphylococcal nuclease: Evidence of substantial electrostatic interactions in the denatured state. Biochemistry. 2000; 39:14292– 14304. [PubMed: 11087378]
- 25. Jones TA, Zhou JY, Cowan SW, Kjeldgaard M. Improved methods for building protein models into electron density maps and the location of errors in these models. Acta Crystallographica A. 1991; 47:110–119.
- 26. Brünger A, Adams P, Clore G, DeLano W, Gros P, Grosse-Kunstleve R, Jiang J, Kuszewski J, Nilges M, Pannu N, Read R, Rice L, Simonson T, Warren G. Crystallography & NMR system: A new software suite for macromolecular structure determination. Acta Crystallographica, Section D: Biological Crystallography. 1998; 54(Pt 5):905–921.
- Isom DG, Cannon BR, Castañeda CA, Robinson A, Garcia-Moreno EB. High tolerance for ionizable residues in the hydrophobic interior of proteins. Proc. Natl. Acad. Sci. USA. 2008; 105:17784–17788. [PubMed: 19004768]
- 28. Su Z, Wu J, Fang H, Tsong T, Chen H. Local stability identification and the role of a key aromatic amino acid residue in staphylococcal nuclease. FEBS Journal. 2005; 272:3960–3966. [PubMed: 16045766]
- Hirano S, Kamikubo H, Yamazaki Y, Kataoka M. Elucidation of information encoded in tryptophan 140 of staphylococcal nuclease. Proteins: Structure, Function, and Bioinformatics. 2005; 58:271–277.
- Baskakov IV, Bolen DW. Monitoring the sizes of denatured ensembles of staphlococcal nuclease proteins: implications regarding m values, intermediates, and thermodynamics. Biochemistry. 1998; 37:18010–18017. [PubMed: 9922169]
- 31. Van Aalten DMF, Crielaard W, Hellingwerf KJ, Joshua-Tor L. Conformational substates in different crystal forms of the photoactive yellow protein Correlation with theoretical and experimental flexibility. Protein Science. 2000; 9:64–72. [PubMed: 10739248]
- 32. Ho M, Menetret J, Tsuruta H, Allen KN. The origin of the electrostatic perturbation in acetoacetate decarboxylase. Nature. 2009; 459:393–399. [PubMed: 19458715]
- 33. Denisov VP, Schlessman JL, Garcia-Moreno EB, Halle B. Stabilization of Internal Charges in a Protein: Water Penetration or Conformational Change? Biophysical J. 2004; 87:3982–3994.
- 34. Dao-pin S, Anderson DE, Baase WA, Dahlquist FW, Matthews BW. Structural and thermodynamic consequences of burying a charged residue within the hydrophobic core of T4 lysozyme. Biochemistry. 1991; 30:11521–11529. [PubMed: 1747370]
- Strajbl M, Shurki A, Warshel A. Converting conformational changes to electrostatic energy in molecular motors: The energetics of ATP synthase. Proc. Natl. Acad. Sci. USA. 2003; 100:14834– 14839. [PubMed: 14657336]

36. Olsson MHM, Warshel A. Monte Carlo simulations of proton pumps: On the working principles of the biological valve that controls proton pumping in cytochrome c oxidase. Proceedings of the National Academy of Sciences USA. 2006; 103:6500–6505.

- 37. Brown LS, Kamikubo H, Zimanyi L, Kataoka M, Tokunaga F, Verdegem P, Lugtenburg J, Lanyi JK. A local electrostatic change is the cause of the large-scale protein conformation shift in bacteriorhodopsin. Proceedings of the National Academy of Sciences USA. 1997; 944:5040–5044.
- 38. Lanyi JK. Crystallographic studies of the conformational changes that drive directional transmembrane ion movement in bacteriorhodopsin. Biochimica et Biophysica Acta. 2000; 1459:339–345. [PubMed: 11004449]
- Song Y, Mao J, Gunner MR. Calculation of Proton Transfers in Bacteriorhodopsin bR and M Intermediates. Biochemistry. 2003; 42:9875–9888. [PubMed: 12924936]
- 40. Rastogi VK, Girvin ME. Structural changes linked to proton translocation by subunit c of the ATPase synthase. Nature. 1999; 402:263–268. [PubMed: 10580496]
- 41. Xie A, Kelemen L, Hendriks J, White BJ, Hellingwerf KJ, Hoff WD. Formation of a New Buried Charge Drives a Large-Amplitude Protein Quake in Photoreceptor Activation. Biochemistry. 2001; 40:1510–1517. [PubMed: 11327809]
- 42. Lee B, Croonquist PA, Sosnick TR, Hoff WD. PAS Domain Receptor Photoactive Yellow Protein Is Converted to a Molten Globule State upon Activation. J. Biol. Chem. 2001; 276:20821–20823. [PubMed: 11319215]
- 43. Hoff WD, Xie A, Van Stokkum IHM, Tang X, Gural J, Kroon AR, Kellingwerf KJ. Global Conformational Changes upon Receptor Stimulation in Phtoactive Yellow Protein. Biochemistry. 1999; 38
- 44. Castañeda CA, Fitch CA, Majumdar A, Khangulov V, Schlessman JL, Garcia-Moreno EB. Molecular determinants of the pKa values of Asp and Glu residues in staphylococcal nuclease. Proteins: Struct. Funct. Bioinf. 2009; 77:570–588.
- 45. Forsyth WR, Gilson MK, Antosiewicz J, Jaren OR, Robertson AD. Theoretical and experimental analysis of ionization equilibria in ovomucoid third domain. Biochemistry. 1998; 37:8643–8652. [PubMed: 9628726]
- 46. Antosiewicz J, Mc Cammon AJ, Gilson MK. The determinants of p $K_a$ s in proteins. Biochemistry. 1996; 35:7819–7833. [PubMed: 8672483]
- 47. Antosiewicz J, McCammon JA, Gilson MK. Prediction of pH-dependent properties of proteins. Journal of Molecular Biology. 1994; 238:415–436. [PubMed: 8176733]
- 48. Georgescu RE, Alexov EG, Gunner MR. Combining conformational flexibility and continuum electrostaics for calculating pKas in proteins. Biophysical Journal. 2002; 83:1731–1748. [PubMed: 12324397]
- 49. Alexov E. Role of the protein side-chain fluctuations on the strength of pair-wise electrostatic interactions: comparing experimental with computed pKas. Proteins: Structure, Function, Genetics. 2003; 50:94–103.
- 50. Kuhn B, Kollman PA, Stahl M. Prediction of p*K*a shifts in proteins using a combination of molecular mechanical and continuum solvent calculations. Journal of Computational Chemistry. 2004; 25:1865–1872. [PubMed: 15376253]
- 51. van Vlijmen HWT, Schaefer M, Karplus M. Improving the accuracy of protein p $K_a$  calculations: Conformational averaging versus the average structure. Proteins: Structure, Function, and Genetics. 1998; 33:145–158.
- 52. Ghosh N, Cui Q. p*K*a of residue 66 in staphylococcal nuclease. I. Insights from QM/MM simulations with conventional sampling. J. Phys. Chem. B. 2008; 112:8387–8397. [PubMed: 18540669]
- Zheng L, Mengen C, Yang W. Random walk in orthogonal space to achieve efficient free-energy simulation of complex systems. Proc. Natl. Acad. Sci. USA. 2008; 105:20227–20232. [PubMed: 19075242]
- 54. Kato M, Warshel A. Using a charging coordinate in studies of ionization induced partial unfolding. J. Phys. Chem. B. 2006; 110:11566–11579. [PubMed: 16771433]
- 55. Khandogin J, Brooks CL. Constant pH molecular dynamics with proton tautomerism. Biophysical J. 2005; 89:141–157.

56. Khandogin J, Brooks CLI. Towards the accurate first-principles prediction of ionization equilibria in proteins. Biochemistry. 2006; 45:9363–9373. [PubMed: 16878971]

DeLano WL. The PyMOL Molecular Graphics System. DeLano Scientific, Palo Alto, CA USA.
 2002

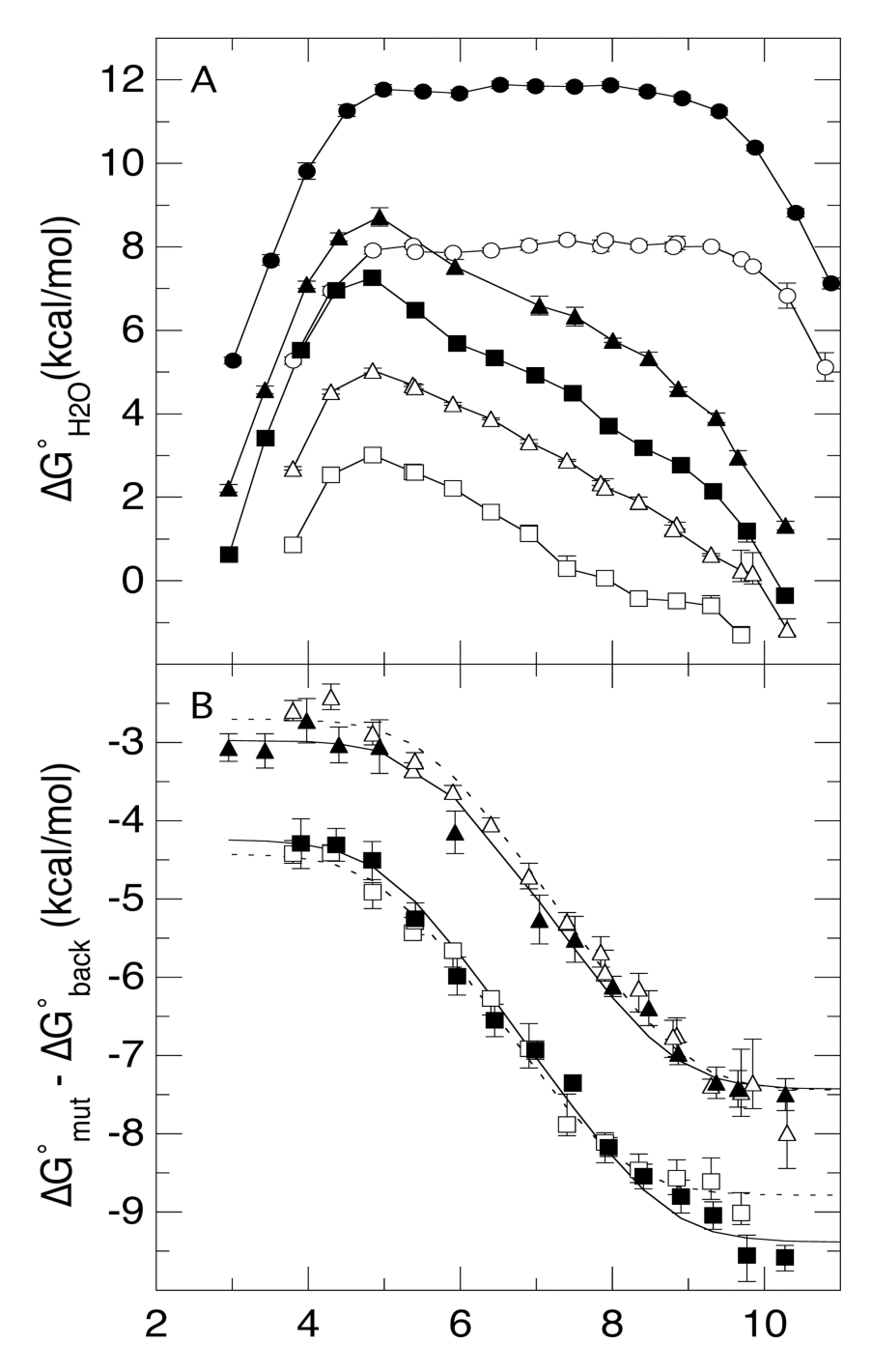


Figure 1. (A) pH dependence of thermodynamic stability  $(\Delta G^{\circ}_{H2O})$  measured by GdmCl denaturation monitored by changes in Trp fluorescence for PHS nuclease ( $\bigcirc$ ) and  $\triangle$ +PHS nuclease ( $\bigcirc$ ), and for V66D ( $\square$ , and V66E ( $\triangle$ ,  $\triangle$ ) variants of these proteins (open symbols for PHS, closed symbols for  $\triangle$ +PHS). All data at 298 K in 100 mM KCl. The error bars represent errors of the fit of individual denaturation experiments. The lines are meant only to guide the eye. (B) Difference in stability ( $\triangle G^{\circ}_{mut}$  -  $\triangle G^{\circ}_{back}$ ) between PHS and its V66D ( $\square$ ) and V66E ( $\triangle$ ) variants, and between  $\triangle$ +PHS and its V66D ( $\square$ ) and V66E ( $\triangle$ ) variants. The

dashed curves through the data represent fits of Equation 3 in Karp et al (10) for the PHS (---) and  $\Delta+PHS$  (----) proteins.

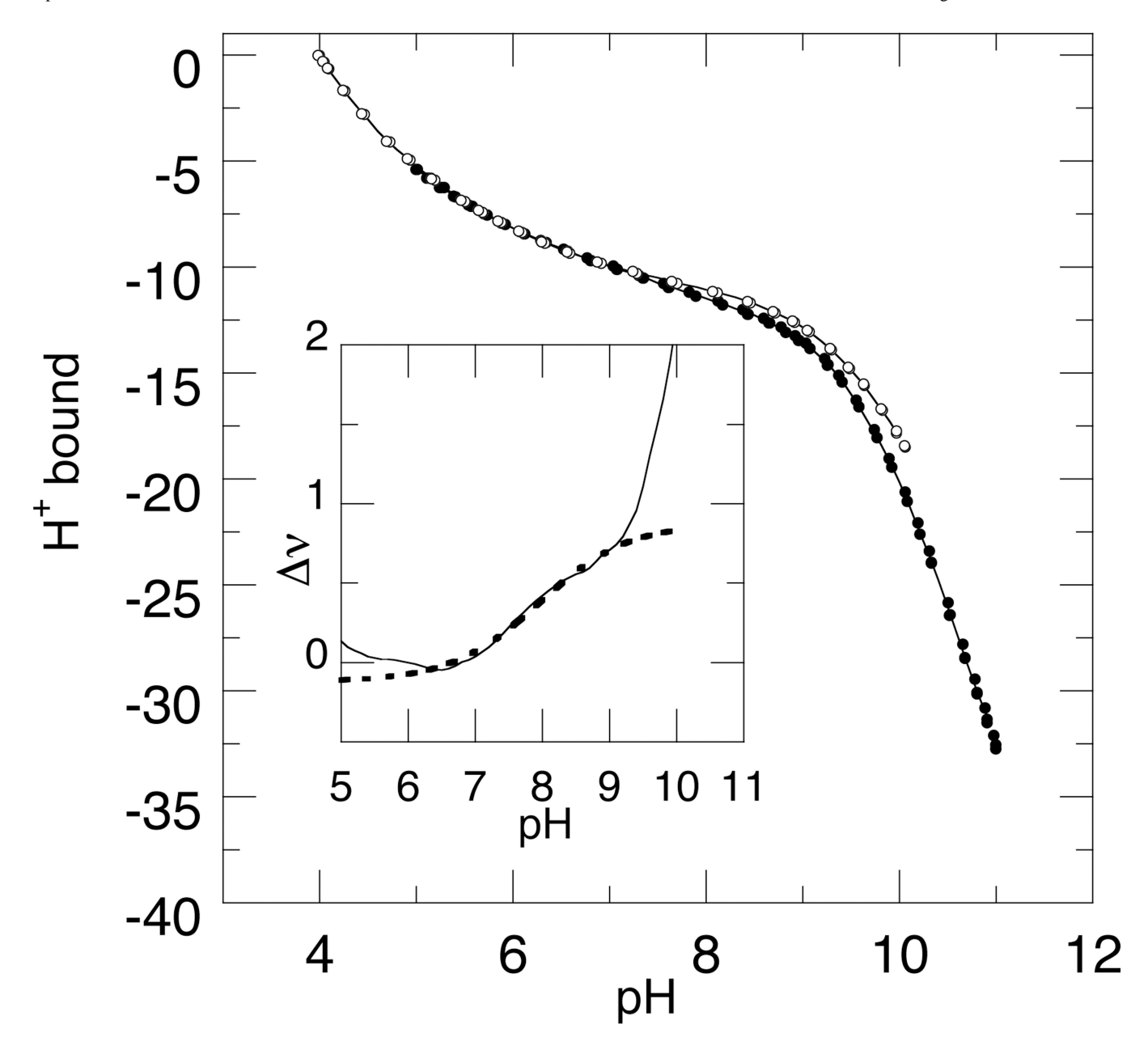


Figure 2. Potentiometric H<sup>+</sup> binding measured with PHS (O) and the PHS/V66D variant (●) at 298 K in 100 mM KCl. The solid lines represent cubic linear interpolation. The solid line in the insert shows the difference between the interpolated curves for these two proteins, and the dotted line represents the fit of Equation 4 from Karp et al. (10), with the amplitude of the titration fixed as 1.

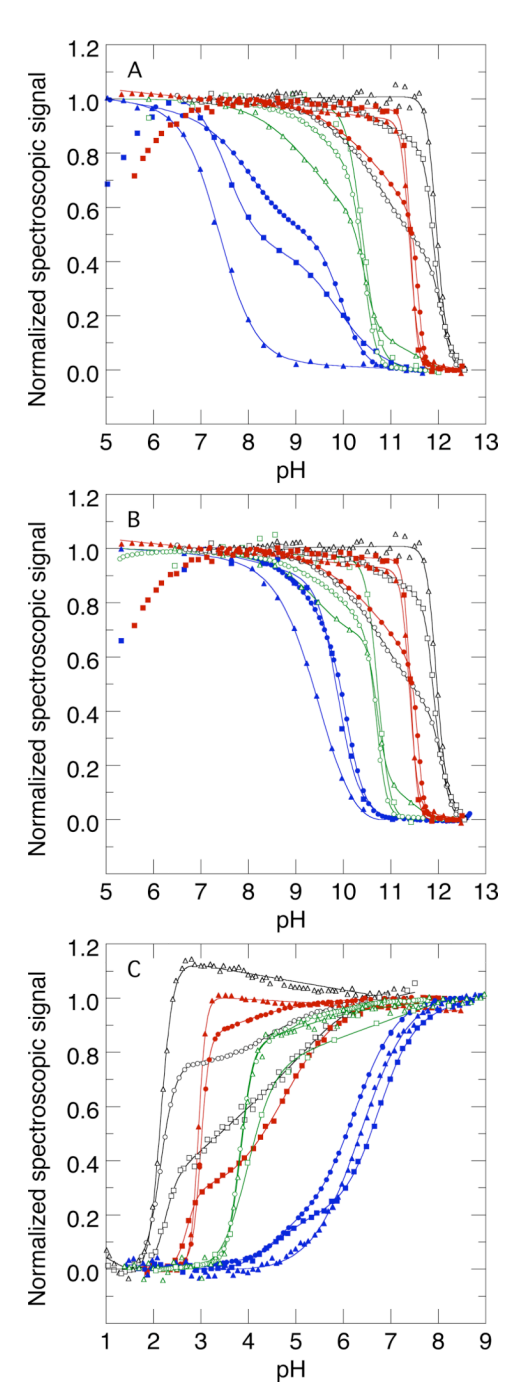
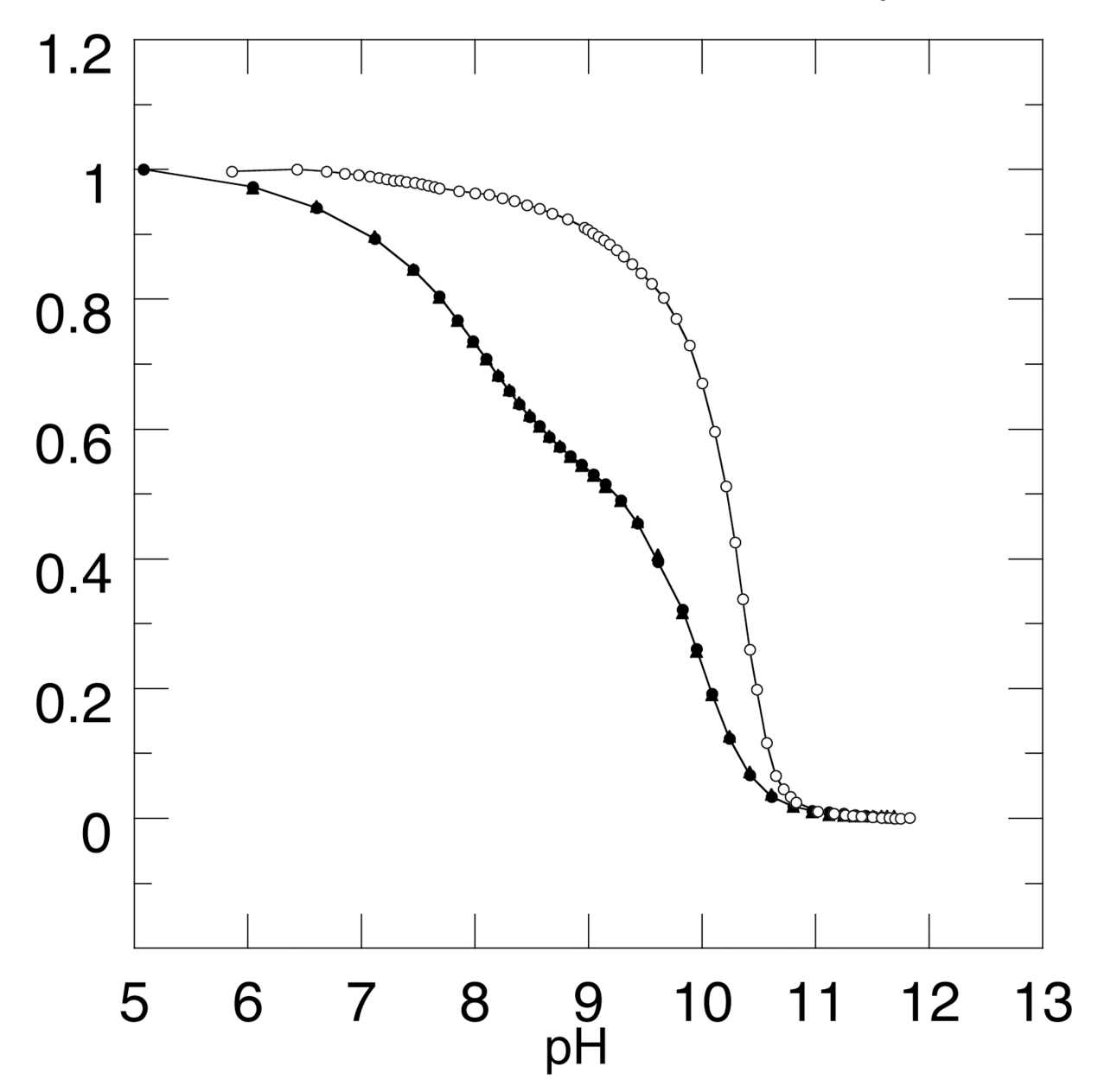


Figure 3. Acid/base titrations monitored by Trp fluorescence  $(\bigcirc, \bullet)$ , far UV-CD at 222 nm  $(\triangle, \blacktriangle)$ , and near UV-CD at 275 nm  $(\square, \blacksquare)$  for variants of PHS of  $\Delta$ +PHS nuclease. The line represents nonlinear square fits of two state (Eq. 1 from Karp et al (10)) or three state (Eq. 2 from Karp et al (10)) models to the data. (A) Base titration of  $\Delta$ +PHS nuclease (black), PHS nuclease (red),  $\Delta$ +PHS/V66D (green) and PHS/V66D (blue). (B) Base titration of  $\Delta$ +PHS nuclease (black), PHS nuclease (red),  $\Delta$ +PHS nuclease (red),  $\Delta$ +PHS/V66E (green) and PHS/V66K (green) and PHS/V66K (blue).





**Figure 4.** Acid/base titration of PHS/V66D in the absence (●) and in the presence (○) of 4 M glycerol, monitored by Trp fluorescence at 298 K.

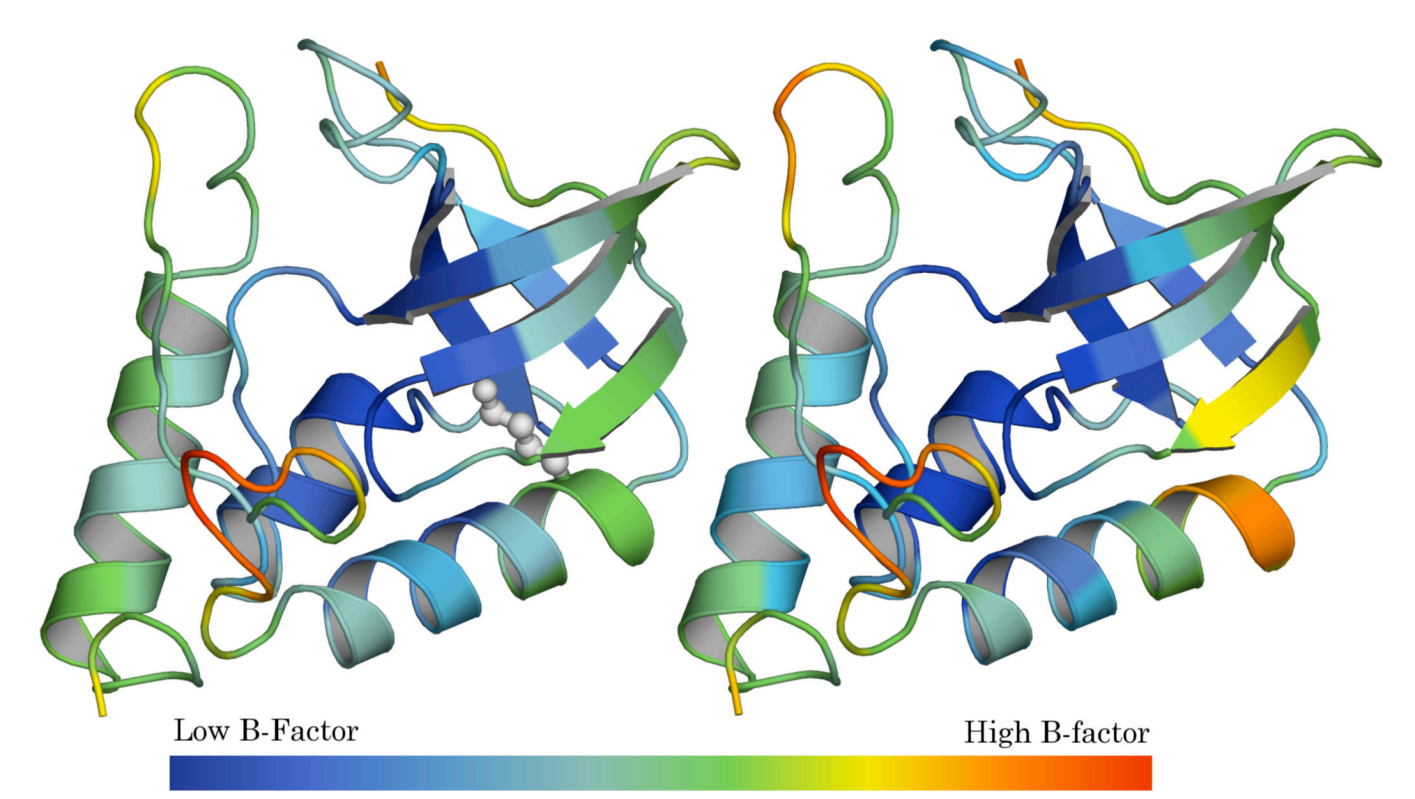


Figure 5.

B factors in the structures of PHS/V66K at pH 7 (left) and pH 4.7 (right). The side chain of Lys-66 is shown as grey spheres in the pH 7 structure. The color bar identifies high and low B factors. Figure drawn with PyMol (57).

Table 1 Summary of p $K_a$  values of Asp-66, Glu-66, and Lys-66 in SNase

| Residue | Background<br>protein     | <sup>4</sup> pK <sub>a</sub> by potentiometry | ${ m p}K_{ m a}$ from chemical denaturation |
|---------|---------------------------|---|---|
| Asp-66  | I <sub>PHS</sub>          | 7.97 (7.85, 8.07)                             | 8.05 (7.86, 8.25)                           |
| Asp-66  | $2_{\Delta+\mathrm{PHS}}$ | 58.95 (8.92, 8.99)                            | <sup>5</sup> 8.73 (8.45, 9.03)              |
| Glu-66  | PHS                       | 68.80 (8.70, 8.90)                            | 8.99 (8.73, 9.28)                           |
| Glu-66  | Δ+PHS                     | 9.07 (9.00, 9.10)                             | 8.80 (8.48, 9.14)                           |
| Lys-66  | PHS                       | <sup>7</sup> 6.35 (6.25, 6.45)                | -   |
| Lys-66  | Δ+PHS                     | <sup>8</sup> 5.63 (5.60, 5.64)                | <sup>8</sup> 5.83 (5.61, 6.05)              |
| Lys-66  | $J_{ m WT}$               | -   | <sup>9</sup> 6.38 (6.01, 6.75)              |

 $<sup>^{</sup>I}\mathrm{Stable}$  form of nuclease engineered with three substitutions: P117G, H124A, and S128L

 $<sup>^2\</sup>mathrm{Stable}$  form of nuclease engineered from PHS with G50F, V51N and a 44–49 deletion.

 $<sup>^{3}</sup>$ Measured with the V66K variant of the wild type protein.

 $<sup>^{4}</sup>$  In the fits the amplitude of the difference  $\mathrm{H}^{+}$  binding curves (insert Fig. 2) was fixed at 1.0.

<sup>5</sup> From Karp et al (10).

From Dwyer et al (11).

<sup>&</sup>lt;sup>7</sup> From Garcia-Moreno et al (8).

<sup>8</sup> From Fitch et al (7).

<sup>9</sup> From Stites et al (9).

Table 2 Equilibrium thermodynamic parameters for acid/base unfolding.

| Variant | Background | Signal                            | $\mathrm{pH}_{\mathrm{mid}}{}^{I}$ | $\mathrm{pH_{mid}}^2$            |
|---------|------------|-----------------------------------|------------------------------------|----------------------------------|
| V66K    | Δ+PHS      | CD ( $\lambda = 222 \text{ nm}$ ) | 5 <sub>4.8</sub> (4.2,5.6)         | 53.86 (3.83,3.88)                |
|         |            | CD ( $\lambda = 275 \text{ nm}$ ) | -                                  | 3.95 (3.82,4.01)                 |
|         |            | Fluorescence                      | <sup>5</sup> 4.92 (4.84,4.99)      | <i>5</i> 3.83 (3.82,3.83)        |
|         | PHS        | CD ( $\lambda = 222 \text{ nm}$ ) | 6.38 (6.31, 6.47)                  | -                                |
|         |            | CD ( $\lambda = 275 \text{ nm}$ ) | 6.72 (6.68, 6.76)                  | 4.47 (4.32,4.63)                 |
|         |            | Fluorescence                      | <sup>3</sup> 6.25 (6.24, 6.26)     | <sup>3</sup> 4.53 (4.49, 4.57)   |
| V66D    | Δ+PHS      | CD ( $\lambda = 222 \text{ nm}$ ) | 6 <sub>9.51</sub> (9.26, 9.74)     | 610.42 (10.39,10.45)             |
|         |            | CD ( $\lambda = 275 \text{ nm}$ ) | -                                  | 6 <sub>10.40</sub> (10.37,10.45) |
|         |            | Fluorescence                      | <sup>6</sup> 9.68 (9.63, 9.72)     | 6 <sub>10.41</sub> (10.40,10.42) |
|         | PHS        | CD ( $\lambda = 222 \text{ nm}$ ) | 7.40 (7.34, 7.47)                  | -                                |
|         |            | CD ( $\lambda = 275 \text{ nm}$ ) | 7.55 (7.50, 7.60)                  | 9.89 (9.81,9.97)                 |
|         |            | Fluorescence                      | 8.10 (8.04, 8.16)                  | 9.97 (9.95,9.99)                 |
| V66E    | Δ+PHS      | CD ( $\lambda = 222 \text{ nm}$ ) | 9.5 (9.2, 9.8)                     | 10.7 (10.67,10.73)               |
|         |            | CD ( $\lambda = 275 \text{ nm}$ ) | -                                  | 10.73 (10.66,10.80)              |
|         |            | Fluorescence                      | 10.18 (10.12, 10.24)               | 10.67 (10.66,10.69)              |
|         | PHS        | CD ( $\lambda = 222 \text{ nm}$ ) | -                                  | 9.59 (9.49,9.70)                 |
|         |            | CD ( $\lambda = 275 \text{ nm}$ ) | -                                  | 9.88 (9.72,10.03)                |
|         |            | Fluorescence                      | <sup>4</sup> 9.44 (9.41, 9.47)     | <sup>4</sup> 10.07 (10.06,10.08) |

<sup>&</sup>lt;sup>1</sup>Midpoint of the minor transition.

 $<sup>^2\!\</sup>mathrm{Midpoint}$  of the cooperative transition corresponding to acid or base unfolding.

 $<sup>^3</sup>$ Data comparable to these were presented previously (8).

 $<sup>^{4}</sup>_{\ \ Data\ comparable\ to\ these\ were\ presented\ previously\ (11).}$ 

<sup>&</sup>lt;sup>5</sup>Data comparable to these were presented previously(7).

<sup>&</sup>lt;sup>6</sup>Data comparable to these were presented previously (10).